Journal of Computational Physics **155,** 178–198 (1999)
Article ID jcph.1999.6336, available online at http://www.idealibrary.com on IDEAL®

A New Discrete Velocity Method for Navier–Stokes Equations

Michael Junk* and S. V. Raghurama Rao†

**Fachbereich Mathematik, Universität Kaiserslautern, D-67663 Kaiserslautern, Germany;*
†Institut für Techno- und Wirtschaftsmathematik, Erwin-Schrödinger-Straße, Kaiserslautern, D-67663 Kaiserslautern, Germany
E-mail: junk@mathematik.uni-kl.de, raghu@itwm.uni-kl.de

Received March 2, 1999; revised June 30, 1999

The relation between the lattice Boltzmann method, which has recently become popular, and the kinetic schemes, which are routinely used in computational fluid dynamics, is explored. A new discrete velocity method for the numerical solution of Navier–Stokes equations for incompressible fluid flow is presented by combining both the approaches. The new scheme can be interpreted as a pseudo-compressibility method and, for a particular choice of parameters, this interpretation carries over to the lattice Boltzmann method.

Key Words: discrete velocity method; lattice Boltzmann method; kinetic schemes; incompressible Navier–Stokes equations; pseudo-compressibility methods.

1. INTRODUCTION

In the last decade, the lattice Boltzmann method has emerged as a potential alternative to other computational fluid dynamics techniques in simulating fluid flows numerically. The lattice Boltzmann method (LBM) was first introduced by McNamara and Zanetti [1] to overcome the drawbacks of the lattice gas cellular automata (LGCA), which resulted from attempts to obtain macroscopic fluid flow simulations from the simplest possible microscopic description using a discrete phase space. See Refs. [2–4] for reviews of the LGCA, Refs. [5, 6] for reviews of the lattice Boltzmann method, and [7] for a review of the related idea of discrete velocity models.

Some authors noted the closeness of the lattice Boltzmann method to the kinetic schemes (see [8, 9]), which, like the lattice Boltzmann method, also use the Boltzmann equation of kinetic theory as the starting point, but are aimed at solving the macroscopic equations of fluid flow (see [10] for a review of kinetic schemes). Both methods exploit the fact that the Boltzmann evolution is essentially equivalent to Euler or Navier–Stokes evolution if the state is in or close to local thermodynamic equilibrium. While most of the kinetic

0021-9991/99 $30.00

schemes were developed and routinely used for the solution of compressible equations, the lattice Boltzmann method operates in the incompressible limit. However, as we will show in Section 2, the two methods even coincide for a particular parameter constellation. This implies that the observations which are valid for kinetic schemes also have a direct consequence on LBM. In view of these remarks it is surprising that the close relation between the two methods is not fully appreciated. Our intention is to stress the remarkable coincidence.

The first kinetic scheme was introduced more than two decades ago, by Sanders and Prendergast [11]. It is popularly known as the *beam scheme*, and, incidentally, is also a discrete velocity method for simulating Euler equations. A few years later, an approach to construct kinetic schemes for general hyperbolic systems of conservation laws was described by Harten *et al*. [12]. Many kinetic schemes for the compressible Euler system based on the original Maxwellian distribution were developed afterwards by Pullin [13], Reitz [14], Deshpande and Mandal [15–17], Perthame and Coron [18, 19], Prendergast and Xu [20], Xu *et al.* [21], and Raghurama Rao and Deshpande [22, 23]. For the isentropic Euler system, Kaniel investigated a kinetic scheme based on an equilibrium distribution function which is different from the classical Maxwellian [24, 25]. A general approach to construct equilibrium distributions has been presented by Junk in [26] and by Perthame [27] who uses an entropy principle. For the compressible Navier–Stokes system, kinetic schemes were developed by Chou and Baganoff [28] and in the group of Deshpande [29, 30]. A slightly different approach was taken by Xu and Prendergast [31].

For scalar conservation laws in one space dimension Bäcker and Dressler found equilibrium distributions following the idea of Kaniel [32]. In arbitrary space dimensions the scalar case could be treated with a slightly modified transport equation [33, 34]. This approach led to a detailed investigation of the relation between the hydrodynamic limit of kinetic equations and nonlinear conservation laws by Lions *et al.* [35].

In this paper, we present a new discrete velocity method based on the methodology of the kinetic schemes. In Section 2, the original concept of kinetic schemes for Euler equations is introduced and then applied with a special equilibrium distribution known from the lattice Boltzmann method. After that, the obtained discrete velocity method is extended to the Navier–Stokes case by constructing a new discrete Chapman–Enskog distribution. In Section 4, consistency of the resulting scheme is investigated, leading to an interpretation of both kinetic schemes and LBM as pseudo-compressibility methods. Section 5 concludes with numerical results and discussions.

2. KINETIC SCHEMES FOR EULER EQUATIONS

2.1. *Traditional Kinetic Schemes in CFD*

The basis of kinetic schemes is the connection between the Boltzmann equation of kinetic theory of gases and the macroscopic equations of fluid flow. The fluid flow equations can be obtained as (velocity) moments of the Boltzmann equation

$$\frac{\partial f}{\partial t} + \mathbf{v} \cdot \nabla f = Q(f). \tag{1}$$

Here $f(\mathbf{x}, \mathbf{v}, t)$ is the velocity distribution function of the gas particles and the gradient is taken with respect to the space variable $\mathbf{x}$. The left hand side of Eq. (1) denotes the

free flow of the molecules. This free flow is disturbed by the molecular collisions, which is represented by the collision term, $Q(f)$, on the right hand side of Eq. (1). The mass, momentum, and energy of the fluid can be obtained as the velocity averages of the particle mass, momentum, and energy densities. Introducing the notation

$$\langle f \rangle = \int_{-\infty}^{\infty} \int_{-\infty}^{\infty} \int_{-\infty}^{\infty} f \, dv_1 \, dv_2 \, dv_3 \tag{2}$$

this can be formulated as

$$\rho = \langle f \rangle, \qquad \rho \mathbf{u} = \langle \mathbf{v} f \rangle, \qquad \rho \epsilon = \left\langle \frac{1}{2} |\mathbf{v}|^2 f \right\rangle. \tag{3}$$

The macroscopic equations can be obtained by integrating the Boltzmann equation (1), after multiplying it by the vector of the moment functions, as

$$\left\langle \begin{pmatrix} 1 \\ \mathbf{v} \\ \frac{1}{2}|\mathbf{v}|^2 \end{pmatrix} \left(\frac{\partial f}{\partial t} + \mathbf{v} \cdot \nabla f - Q(f) \right) \right\rangle = 0. \tag{4}$$

Using (3), we get the system

$$\begin{aligned} \frac{\partial \rho}{\partial t} + \operatorname{div} \rho \mathbf{u} &= \langle Q \rangle \\ \frac{\partial (\rho \mathbf{u})}{\partial t} + \operatorname{div} \langle \mathbf{v} \otimes \mathbf{v} f \rangle &= \langle \mathbf{v} Q \rangle \\ \frac{\partial (\rho \epsilon)}{\partial t} + \operatorname{div} \left\langle \frac{1}{2} |\mathbf{v}|^2 \mathbf{v} f \right\rangle &= \left\langle \frac{1}{2} |\mathbf{v}|^2 Q \right\rangle. \end{aligned} \tag{5}$$

The mass, momentum, and energy are conserved during collisions. Therefore, we have

$$\langle Q \rangle = 0, \qquad \langle \mathbf{v} Q \rangle = 0, \qquad \left\langle \frac{1}{2} |\mathbf{v}|^2 Q \right\rangle = 0. \tag{6}$$

Substituting (6) in (5) we obtain

$$\begin{aligned} \frac{\partial \rho}{\partial t} + \operatorname{div} \rho \mathbf{u} &= 0 \\ \frac{\partial (\rho \mathbf{u})}{\partial t} + \operatorname{div} \langle \mathbf{v} \otimes \mathbf{v} f \rangle &= 0 \\ \frac{\partial (\rho \epsilon)}{\partial t} + \operatorname{div} \left\langle \frac{1}{2} |\mathbf{v}|^2 \mathbf{v} f \right\rangle &= 0. \end{aligned} \tag{7}$$

In the Euler limit, the gas is dominated by collisions and the particle distribution attains the form of a Maxwellian, given by

$$\mathcal{M}(v) = \frac{\rho}{(2\pi T)^{\frac{3}{2}}} \exp\left(-\frac{|\mathbf{v} - \mathbf{u}|^2}{2T} \right). \tag{8}$$

This velocity distribution is well known as the one of a gas in (local) thermodynamic equilibrium. Hence, the Maxwellian is also called the *equilibrium distribution*. When the distribution is a Maxwellian, the fluxes in (7) can be calculated, yielding

$$\langle \mathbf{v} \otimes \mathbf{v}\mathcal{M} \rangle = \rho \mathbf{u} \otimes \mathbf{u} + \rho T I \qquad \text{and} \qquad \left\langle \frac{1}{2}|\mathbf{v}|^2 \mathbf{v}\mathcal{M} \right\rangle = \rho(\epsilon + T)\mathbf{u}, \tag{9}$$

where I is the identity matrix. Using the above, we obtain the Euler equations as

$$\begin{aligned} \frac{\partial \rho}{\partial t} + \operatorname{div}(\rho \mathbf{u}) &= 0 \\ \frac{\partial(\rho \mathbf{u})}{\partial t} + \operatorname{div}(\rho \mathbf{u} \otimes \mathbf{u} + \rho T I) &= 0 \\ \frac{\partial(\rho \epsilon)}{\partial t} + \operatorname{div}(\rho(\epsilon + T)\mathbf{u}) &= 0 \end{aligned} \tag{10}$$

or equivalently in the form

$$\left\langle \begin{pmatrix} 1 \\ \mathbf{v} \\ \frac{1}{2}|\mathbf{v}|^2 \end{pmatrix} \left(\frac{\partial f}{\partial t} + \mathbf{v} \cdot \nabla f \right) \right\rangle = 0, \qquad f = \mathcal{M}. \tag{11}$$

While standard discretizations of the Euler system are based on (10), kinetic schemes use the representation (11) which is motivated by kinetic theory. An obvious advantage of (11) is the much simpler differential operator which is linear and scalar in contrast to the more complicated nonlinear system (10).

To discretize (11), traditional CFD techniques like finite difference, finite volume, finite element, or spectral methods can be applied. Equivalently, one can use the *Lagrangian approach*. In this approach, we replace (11) by the auxiliary problem

$$\frac{\partial f}{\partial t} + \mathbf{v} \cdot \nabla f = 0, \qquad f|_{t=0} = \mathcal{M} \tag{12}$$

for which the solution is straightforward, given by

$$f(\mathbf{x}, \mathbf{v}, t) = f(\mathbf{x} - \mathbf{v}t, \mathbf{v}, 0). \tag{13}$$

Clearly, this solution satisfies

$$\left\langle \begin{pmatrix} 1 \\ \mathbf{v} \\ \frac{1}{2}|\mathbf{v}|^2 \end{pmatrix} \left(\frac{\partial f}{\partial t} + \mathbf{v} \cdot \nabla f \right) \right\rangle = 0.$$

However, the constraint $f = \mathcal{M}$ is enforced only initially. The violation of this constraint leads to an increasing error as time increases. By stopping the evolution after a small time step Δt and restarting it with a Maxwellian (that has the same ρ, u, ϵ-moments as the solution of the just finished free flow step), the error can be kept of order Δt, giving rise to a first order method for the Euler equations. Thus, two clear steps can be identified for the Lagrangian approach: a convection step and a relaxation step. In the relaxation step, the velocity distribution relaxes completely to the equilibrium distribution.

2.2. *Kinetic Schemes with Discrete Distributions*

While the kinetic schemes mentioned in the above subsection are designed to solve the Euler system, it is not necessary to be limited by this restriction. Also, the choice of $\mathcal{M}$ as equilibrium constraint is not mandatory. Obviously, the approach is applicable whenever the system of equations allows a representation of type (11). In the following, we are going to restrict our considerations to the case of isothermal Euler equations, in order to work out the similarities with the lattice Boltzmann method. The isothermal equations (with $T = T_0 = c_s^2$ where c_s is the sound speed) are of the form

$$\begin{aligned} \frac{\partial \rho}{\partial t} + \operatorname{div}(\rho \mathbf{u}) &= 0 \\ \frac{\partial (\rho \mathbf{u})}{\partial t} + \operatorname{div}\big(\rho \mathbf{u} \otimes \mathbf{u} + c_s^2 \rho I\big) &= 0 \end{aligned} \tag{14}$$

or equivalently

$$\left\langle \begin{pmatrix} 1 \\ \mathbf{v} \end{pmatrix} \left(\frac{\partial f}{\partial t} + \mathbf{v} \cdot \nabla f \right) \right\rangle = 0, \qquad f = \mathcal{M}|_{T=T_0}. \tag{15}$$

Instead of the classical Maxwellian $\mathcal{M}$ (with fixed temperature $T = T_0$), we can also choose any distribution F, as long as the integral expressions in (15) together with the constraint $f = F$ are equivalent to the Euler system (14). Since the integral involves velocity moments up to second order, we are led to the following compatibility conditions on the equilibrium distribution

$$\begin{aligned} \langle F \rangle &= \rho \\ \langle \mathbf{v} F \rangle &= \rho \mathbf{u} \\ \langle \mathbf{v} \otimes \mathbf{v} F \rangle &= \rho \mathbf{u} \otimes \mathbf{u} + c_s^2 \rho I. \end{aligned} \tag{16}$$

In particular, we are interested in discrete velocity distributions F which satisfy these moment constraints (see also the works of Sanders and Prendergast [11], Nadiga and Pullin [36], and M. Junk [37, 38]. An explicit example in 2D is given by the so-called D2Q9 distribution used in the lattice Boltzmann method. It is of the form

$$F(\rho, \mathbf{u}; \mathbf{v}) = \sum_{i=0}^{8} F_i(\rho, \mathbf{u})\, \delta(\mathbf{v} - \mathbf{v}_i), \tag{17}$$

where δ is the Dirac-delta function and

$$\begin{aligned} \mathbf{v}_0 &= 0 \\ \mathbf{v}_i &= \sqrt{3} c_s \big(\cos\big((i-1)\tfrac{\pi}{2}\big), \sin\big((i-1)\tfrac{\pi}{2}\big)\big)^T, \qquad i = 1, \ldots, 4 \\ \mathbf{v}_i &= \sqrt{6} c_s \big(\cos\big(\big(i-\tfrac{9}{2}\big)\tfrac{\pi}{2}\big), \sin\big(\big(i-\tfrac{9}{2}\big)\tfrac{\pi}{2}\big)\big)^T, \qquad i = 5, \ldots, 8. \end{aligned} \tag{18}$$

The weights F_i are given by

$$F_i(\rho, \mathbf{u}) = F_i^* \rho \left(1 - \frac{1}{2c_s^2} |\mathbf{u}|^2 + \frac{1}{c_s^2} \mathbf{u} \cdot \mathbf{v}_i + \frac{1}{2c_s^4} (\mathbf{u} \cdot \mathbf{v}_i)^2 \right) \tag{19}$$

with

$$F_0^* = \frac{4}{9}, \qquad F_i^* = \frac{1}{9} \text{ for } i = 1, \ldots, 4, \qquad F_i^* = \frac{1}{36} \text{ for } i = 5, \ldots, 8. \tag{20}$$

In order to obtain a kinetic scheme for the isothermal Euler equations, we will approximate the equivalent form

$$\left\langle \begin{pmatrix} 1 \\ \mathbf{v} \end{pmatrix} \left(\frac{\partial f}{\partial t} + \mathbf{v} \cdot \nabla f \right) \right\rangle = 0, \qquad f = F \tag{21}$$

with the Lagrangian approach described in the last section. Solving the free flow equation $\frac{\partial f}{\partial t} + \mathbf{v} \cdot \nabla f = 0$, starting at time t with equilibrium $f(\mathbf{x}, \mathbf{v}, t) = F(\rho(\mathbf{x}, t), \mathbf{u}(\mathbf{x}, t); \mathbf{v})$, yields after a time step Δt

$$\begin{aligned} f(\mathbf{x}, \mathbf{v}, t + \Delta t) &= F(\rho(\mathbf{x} - \mathbf{v}\Delta t, t), \mathbf{u}(\mathbf{x} - \mathbf{v}\Delta t, t); \mathbf{v}) \\ &= \sum_{i=0}^{8} F_i(\rho(\mathbf{x} - \mathbf{v}\Delta t, t), \mathbf{u}(\mathbf{x} - \mathbf{v}\Delta t, t))\delta(\mathbf{v} - \mathbf{v}_i). \end{aligned}$$

Using the relation $\psi(\mathbf{v})\delta(\mathbf{v} - \mathbf{v}_i) = \psi(\mathbf{v}_i)\delta(\mathbf{v} - \mathbf{v}_i)$, which holds for any continuous function ψ, we obtain further

$$f(\mathbf{x}, \mathbf{v}, t + \Delta t) = \sum_{i=0}^{8} F_i(\rho(\mathbf{x} - \mathbf{v}_i\Delta t, t), \mathbf{u}(\mathbf{x} - \mathbf{v}_i\Delta t, t))\delta(\mathbf{v} - \mathbf{v}_i).$$

Denoting the weights of the discrete distribution $f(\mathbf{x}, \mathbf{v}, t + \Delta t)$ by $f_i(\mathbf{x}, t + \Delta t)$, the evolution can also be described without mentioning the Dirac deltas at the (fixed) discrete velocities

$$f_i(\mathbf{x}, t + \Delta t) = F_i(\rho(\mathbf{x} - \mathbf{v}_i\Delta t, t), \mathbf{u}(\mathbf{x} - \mathbf{v}_i\Delta t, t)), \qquad i = 0, \ldots, 8. \tag{22}$$

Since integer multiples of $\mathbf{v}_i\Delta t$ make up a regular square grid which is invariant under $\mathbf{v}_i\Delta t$-translations, the scheme (22) only accesses nodal data if $\mathbf{x}$ is also a node of the grid. We remark that the grid length is given by

$$\Delta x = \sqrt{3} c_s \Delta t. \tag{23}$$

The connection between (22) and the classical lattice Boltzmann method becomes most obvious under the change of variables $\mathbf{x} \mapsto \mathbf{x} + \mathbf{v}_i\Delta t$, which leads to

$$f_i(\mathbf{x} + \mathbf{v}_i\Delta t, t + \Delta t) = F_i(\rho(\mathbf{x}, t), \mathbf{u}(\mathbf{x}, t)), \qquad i = 0, \ldots, 8. \tag{24}$$

Indeed, (24) coincides with the lattice Boltzmann evolution [39, 40]

$$f_i(\mathbf{x} + \mathbf{v}_i\Delta t, t + \Delta t) - f_i(\mathbf{x}, t) = \frac{\Delta t}{t_R}(F_i(\mathbf{x}, t) - f_i(\mathbf{x}, t)) \tag{25}$$

if we set $t_R = \Delta t$ (see Refs. [39, 40] for the LBM based on the BGK-model). At first glance, this seems to be a contradiction, because the kinetic scheme has been set up for the

Euler system while it is known that the lattice Boltzmann method approximates the Navier–Stokes system. In fact, setting $t_R = \Delta t$ amounts to a high dose of viscosity (typically, LBM applications are run with t_R in-between $\frac{1}{2}\Delta t$ and Δt). The apparent contradiction is resolved with the remark that the Lagrangian approach to kinetic schemes yields only a first order method. The numerical viscosity of that scheme is quite high, particularly in applications with low Mach number flows. This numerical viscosity of the kinetic scheme is exactly the viscosity corresponding to $t_R = \Delta t$ in LBM and thus has a physically correct structure. In [38], a kinetic scheme for the Euler system could therefore be used as solver for the Navier–Stokes equations. Huang *et al*. [41], in their lattice Boltzmann method for compressible flows, used a similar approach, even though they did not mention kinetic schemes.

3. EXTENSION TO NAVIER–STOKES EQUATIONS

Kinetic schemes can also be extended to the case of Navier–Stokes equations, by using a Chapman–Enskog distribution function $\mathcal{F}_{CE}$ instead of the Maxwellian constraint $\mathcal{M}$ in (15). This approach has been pursued in [28–30]. The Chapman–Enskog distribution function $\mathcal{F}_{CE}$ is obtained as a small perturbation of the Maxwellian. See Refs. [42, 43, 15, 44] for details of the derivation. For a mono-atomic gas in three dimensions, the distribution function is of the form

$$\mathcal{F}_{CE} = \mathcal{M}\left[1 - \frac{P_{ij}}{p}\frac{1}{2T}c_i c_j - \frac{q_i}{p}\frac{1}{T}c_i\left(1 - \frac{2}{5}\frac{c^2}{2T}\right)\right], \tag{26}$$

where

$$q_i = -K\frac{\partial T}{\partial x_i}, \qquad P_{ij} = -\mu\left(\frac{\partial u_i}{\partial x_j} + \frac{\partial u_j}{\partial x_i} - \frac{2}{3}\delta_{ij}\frac{\partial u_k}{\partial x_k}\right) \tag{27}$$

and $\mathbf{c} = \mathbf{v} - \mathbf{u}$ is the peculiar velocity. Here, we will again consider the simpler case of isothermal equations in 2D. Following [45, 37], the equations are of the form

$$\begin{aligned} \frac{\partial \rho}{\partial t} + \operatorname{div}(\rho\mathbf{u}) &= 0, \\ \frac{\partial(\rho\mathbf{u})}{\partial t} + \operatorname{div}\left(\rho\mathbf{u}\otimes\mathbf{u} + c_s^2\rho I\right) &= \operatorname{div}\eta, \end{aligned} \tag{28}$$

where the viscous stress tensor is given by

$$\eta = \nu\rho(2S + (\operatorname{div}\mathbf{u})I), \qquad S_{ij} = \frac{1}{2}\left(\frac{\partial u_i}{\partial x_j} + \frac{\partial u_j}{\partial x_i}\right).$$

(Note that div η is the vector obtained by applying divergence to the rows of η.) Equivalently, we can write system (28) as

$$\left\langle \begin{pmatrix} 1 \\ \mathbf{v} \end{pmatrix}\left(\frac{\partial f}{\partial t} + \mathbf{v}\cdot\nabla f\right)\right\rangle = 0, \qquad f = F_{CE}, \tag{29}$$

where F_{CE} satisfies the moment constraints

$$\begin{aligned} \langle F_{CE}\rangle &= \rho \\ \langle \mathbf{v} F_{CE}\rangle &= \rho \mathbf{u} \\ \langle \mathbf{v}\otimes\mathbf{v} F_{CE}\rangle &= \rho \mathbf{u}\otimes\mathbf{u} + c_s^2 \rho I - \eta. \end{aligned} \tag{30}$$

Instead of using the continuous distribution function $\mathcal{F}_{CE}$ (given in (26) with $q_i = 0$ and $T = T_0$), we construct a discrete $\mathcal{F}_{CE}$ satisfying (30). One possibility is to discretize the classical Chapman–Enskog distribution function in the velocity variable. A kinetic scheme based on this approach will be presented elsewhere [46]. Here, we follow a different idea based on a general solution technique for moment problems of the form (30) which uses orthogonal polynomials [26]. For the special D2Q9 model, however, it is not necessary to work out the general ideas. In fact, conditions (30) can be reduced to those of the Euler system if we replace $\rho\mathbf{u}\otimes\mathbf{u}$ by $\rho\mathbf{u}\otimes\mathbf{u} - \eta$. This observation can be used, if we write the weights (19) of the equilibrium distribution function (17) in terms of $\rho\mathbf{u}\otimes\mathbf{u}$. Introducing the matrix product

$$A : B = \sum_{i,j=1}^{2} A_{ij} B_{ij}$$

we find

$$\mathbf{u}\otimes\mathbf{u} : \mathbf{v}\otimes\mathbf{v} = \sum_{i,j=1}^{2} u_i u_j v_i v_j = (\mathbf{u}\cdot\mathbf{v})^2$$

and

$$\mathbf{u}\otimes\mathbf{u} : I = \sum_{i,j=1}^{2} u_i u_j \delta_{ij} = |\mathbf{u}|^2$$

so that (19) can be written as

$$F_i(\rho,\mathbf{u}) = F_i^*\rho\left(1 + \frac{1}{c_s^2}\mathbf{u}\cdot\mathbf{v}_i + \frac{1}{2c_s^2}\mathbf{u}\otimes\mathbf{u} : \left(\frac{1}{c_s^2}\mathbf{v}_i\otimes\mathbf{v}_i - I\right)\right).$$

Replacing $\mathbf{u}\otimes\mathbf{u}$ by $\mathbf{u}\otimes\mathbf{u} - \nu(2S + \operatorname{div}\mathbf{u} I)$, we finally obtain

$$\begin{aligned} &F_{CE,i}(\rho,\mathbf{u}) \\ &\quad = F_i^*\rho\left(1 + \frac{1}{c_s^2}\mathbf{u}\cdot\mathbf{v}_i + \frac{1}{2c_s^2}(\mathbf{u}\otimes\mathbf{u} - 2\nu S - \nu \operatorname{div}\mathbf{u} I) : \left(\frac{1}{c_s^2}\mathbf{v}_i\otimes\mathbf{v}_i - I\right)\right), \end{aligned} \tag{31}$$

or after going back to scalar products in $\mathbf{v}_i$ and $\mathbf{u}$,

$$\begin{aligned} F_{CE,i}(\rho,\mathbf{u}) = F_i^*\rho\Bigg(1 &+ \frac{1}{c_s^2}\mathbf{u}\cdot\mathbf{v}_i - \frac{1}{2c_s^2}|\mathbf{u}|^2 + \frac{1}{2c_s^4}(\mathbf{u}\cdot\mathbf{v}_i)^2 \\ &- \frac{\nu}{c_s^4} S : \mathbf{v}_i\otimes\mathbf{v}_i - \frac{\nu}{c_s^2}\operatorname{div}\mathbf{u}\left(\frac{1}{2c_s^2}|\mathbf{v}_i|^2 - 2\right)\Bigg). \end{aligned} \tag{32}$$

It is easy to check that the so defined Chapman–Enskog distribution

$$F_{CE}(\rho, \mathbf{u}; \mathbf{v}) = \sum_{i=0}^{8} F_{CE,i}(\rho, \mathbf{u})\delta(\mathbf{v} - \mathbf{v}_i) \tag{33}$$

satisfies (30). We also remark that F_{CE} is a perturbation of the original D2Q9 equilibrium distribution, similar to the classical case in kinetic theory where (26) is a perturbation of the Maxwellian (8).

To develop a kinetic scheme for Navier–Stokes equations, we follow the same procedure as in the previous section, except that the distribution used as constraint after every time-step will now be the Chapman–Enskog distribution, F_{CE}. We end up with the scheme

$$f_i(\mathbf{x}, t + \Delta t) = F_{CE,i}(\rho(\mathbf{x} - \mathbf{v}_i\Delta t, t), \mathbf{u}(\mathbf{x} - \mathbf{v}_i\Delta t, t)), \qquad i = 0, \ldots, 8, \tag{34}$$

where the moments are updated according to

$$\begin{aligned} \rho(\mathbf{x}, t + \Delta t) &= \sum_{i=0}^{8} f_i(\mathbf{x}, t + \Delta t) \\ \mathbf{u}(\mathbf{x}, t + \Delta t) &= \frac{1}{\rho(\mathbf{x}, t + \Delta t)} \sum_{i=0}^{8} \mathbf{v}_i\, f_i(\mathbf{x}, t + \Delta t). \end{aligned} \tag{35}$$

4. THE INCOMPRESSIBLE LIMIT

To investigate the behavior of the kinetic scheme at low Mach numbers, we first scale the compressible Navier–Stokes system appropriately. Low Mach number flows appear if $\mathbf{u}$ is very small compared to c_s. Taking a typical speed U and length scale L of the flow, the time scale Θ is chosen in accordance to these scales as

$$\Theta = \frac{L}{U}.$$

The density ρ is assumed to be of order one so that no scaling is needed. To avoid superscripts, we will not change the symbols for scaled functions and variables. If we refer to unscaled quantities (which appear less often in this section), we add a hat to the symbols. After some algebra, we obtain the scaled version of (28)

$$\begin{aligned} \frac{\partial \rho}{\partial t} + \frac{\Theta U}{L}\mathrm{div}(\rho\mathbf{u}) &= 0, \\ \frac{\partial(\rho\mathbf{u})}{\partial t} + \frac{\Theta U}{L}\mathrm{div}(\rho\mathbf{u}\otimes\mathbf{u}) + \frac{c_s^2\Theta}{LU}\nabla\rho &= \frac{\Theta}{L^2}\mathrm{div}\,\eta. \end{aligned}$$

By assumption, $\Theta U/L = 1$ and $c_s^2\Theta/(LU) = c_s^2/U^2$. Introducing the Mach number $\mathrm{Ma} = U/c_s$ and the Reynolds number $\mathrm{Re} = UL/\nu$ of the flow, we end up with

$$\begin{aligned} \frac{\partial \rho}{\partial t} + \mathrm{div}(\rho\mathbf{u}) &= 0, \\ \frac{\partial(\rho\mathbf{u})}{\partial t} + \mathrm{div}(\rho\mathbf{u}\otimes\mathbf{u}) + \frac{1}{\mathrm{Ma}^2}\nabla\rho &= \frac{1}{\mathrm{Re}}\mathrm{div}(2\rho S + \rho\,\mathrm{div}\,\mathbf{u} I). \end{aligned} \tag{36}$$

If we approximate (36) by the kinetic scheme introduced in (34), then the time step is related to the grid length by $\Delta\hat{t} = \Delta\hat{x}/(\sqrt{3}c_s)$ (see (23)), or in scaled quantities

$$\Delta t = \frac{1}{\sqrt{3}}\mathrm{Ma}\Delta x. \tag{37}$$

This relation already indicates the typical problem that any explicit solver for the compressible equations faces in the incompressible limit: to get a reasonable space resolution, the time resolution must be extremely fine (if $\mathrm{Ma} \ll 1$) to satisfy the CFL-condition (37).

To find out which equations are approximated by the kinetic scheme, we perform a consistency analysis in the coupled limit $\Delta t, \mathrm{Ma} \to 0$. More precisely, we assume

$$\frac{\Delta t}{\mathrm{Ma}^2} = \lambda = \mathrm{const} \qquad \text{for } \Delta t \to 0, \mathrm{Ma} \to 0. \tag{38}$$

To begin with, let us rewrite the Chapman–Enskog distribution (31) in scaled quantities.

$$F_{CE,i}(\rho, \mathbf{u}) = F_i^* \rho \left(1 + \mathrm{Ma}^2 \mathbf{u}\cdot\mathbf{v}_i + \frac{\mathrm{Ma}^2}{2}\left(\mathbf{u}\otimes\mathbf{u} - \frac{1}{\mathrm{Re}}(2S + \operatorname{div}\mathbf{u} I)\right) : \left(\mathrm{Ma}^2 \mathbf{v}_i \otimes \mathbf{v}_i - I\right)\right). \tag{39}$$

Setting $F_{CE}(\rho, \mathbf{u}; \mathbf{v}) = \sum_{i=0}^{8} F_{CE,i}(\rho, \mathbf{u})\delta(\mathbf{v} - \mathbf{v}_i)$ and using $\rho(\mathbf{x})$ and $\mathbf{u}(\mathbf{x})$ as initial values, the kinetic scheme yields at the end of the first time step

$$\rho^1(\mathbf{x}) = \langle F_{CE}(\rho(\mathbf{x} - \mathbf{v}\Delta t), \mathbf{u}(\mathbf{x} - \mathbf{v}\Delta t); \mathbf{v})\rangle \tag{40}$$

and

$$(\rho^1\mathbf{u}^1)(\mathbf{x}) = \langle \mathbf{v} F_{CE}(\rho(\mathbf{x} - \mathbf{v}\Delta t), \mathbf{u}(\mathbf{x} - \mathbf{v}\Delta t); \mathbf{v})\rangle. \tag{41}$$

To obtain a Taylor expansion around $\Delta t = 0$ we need Δt-derivatives of (40) and (41) up to a certain order. Obviously, each Δt-derivative leads to a space derivative with $-\mathbf{v}$ as factor (i.e., $\partial/\partial\Delta t = -v_i(\partial/\partial x_i)$). To get first order consistency in Δt, we nevertheless need higher Δt-derivatives. This is due to the fact that terms of the form $\Delta t^2/\mathrm{Ma}^2$, $\Delta t^2/\mathrm{Ma}^3$, and $\Delta t^3/\mathrm{Ma}^4$ are not negligible in the coupled limit (38). Consequently, we also need higher order $\mathbf{v}$-moments of the Chapman–Enskog distribution. Taking the scaling into account, we get from (30)

$$\begin{aligned} \langle F_{CE}\rangle &= \rho \\ \langle \mathbf{v} F_{CE}\rangle &= \rho\mathbf{u} \\ \langle \mathbf{v}\otimes\mathbf{v} F_{CE}\rangle &= \rho\mathbf{u}\otimes\mathbf{u} + \frac{1}{\mathrm{Ma}^2}\rho I - \frac{1}{\mathrm{Re}}(2\rho S + \rho \operatorname{div}\mathbf{u} I). \end{aligned} \tag{42}$$

The third order moment can be calculated using the explicit form of F_{CE} given in (39). We find

$$\langle v_i v_j v_k F_{CE}\rangle = \frac{1}{\mathrm{Ma}^2}\rho(\delta_{ij}u_k + \delta_{ik}u_j + \delta_{kj}u_i). \tag{43}$$

Finally, from the fourth and fifth order moments we only need to know the terms of leading order

$$\begin{aligned}\langle v_i v_j v_k v_l F_{CE}\rangle &= \frac{1}{\mathrm{Ma}^4}\rho(\delta_{ij}\delta_{kl}+\delta_{ik}\delta_{jl}+\delta_{il}\delta_{jk})+\mathcal{O}\left(\frac{1}{\mathrm{Ma}^2}\right)\\ \langle v_i v_j v_k v_l v_m F_{CE}\rangle &= \mathcal{O}\left(\frac{1}{\mathrm{Ma}^4}\right).\end{aligned} \tag{44}$$

The Taylor expansion of (40) is then given by

$$\begin{aligned}\rho^1 = \langle F_{CE}\rangle &- \frac{\partial}{\partial x_i}\langle v_i F_{CE}\rangle\Delta t + \frac{1}{2}\frac{\partial^2}{\partial x_i \partial x_j}\langle v_i v_j F_{CE}\rangle\Delta t^2\\ &- \frac{1}{6}\frac{\partial^3}{\partial x_i \partial x_j \partial x_k}\langle v_i v_j v_k F_{CE}\rangle\Delta t^3 + \cdots.\end{aligned}$$

Since

$$\begin{aligned}\langle v_i v_j F_{CE}\rangle\Delta t^2 &= \frac{\Delta t^2}{\mathrm{Ma}^2}\rho\delta_{ij}+\mathcal{O}(\Delta t^2)\\ \langle v_i v_j v_k F_{CE}\rangle\Delta t^3 &= \mathcal{O}\left(\frac{\Delta t^3}{\mathrm{Ma}^2}\right)=\mathcal{O}(\Delta t^2)\\ \langle v_i v_j v_k v_l F_{CE}\rangle\Delta t^4 &= \mathcal{O}\left(\frac{\Delta t^4}{\mathrm{Ma}^4}\right)=\mathcal{O}(\Delta t^2)\end{aligned} \tag{45}$$

we conclude

$$\rho^1 = \rho + \left(\frac{1}{2}\lambda\Delta\rho - \mathrm{div}(\rho\mathbf{u})\right)\Delta t + \mathcal{O}(\Delta t^2). \tag{46}$$

Similarly, we get for the momentum defined in (41)

$$\begin{aligned}(\rho^1\mathbf{u}^1)_l = \langle v_l F_{CE}\rangle &- \frac{\partial}{\partial x_i}\langle v_i v_l F_{CE}\rangle\Delta t + \frac{1}{2}\frac{\partial^2}{\partial x_i \partial x_j}\langle v_i v_j v_l F_{CE}\rangle\Delta t^2\\ &- \frac{1}{6}\frac{\partial^3}{\partial x_i \partial x_j \partial x_k}\langle v_i v_j v_k v_l F_{CE}\rangle\Delta t^3 + \cdots.\end{aligned}$$

While the second order moments yield exactly the fuxes of momentum, the third order moments give rise to some additional terms. Using (43),

$$\frac{1}{2}\frac{\partial^2}{\partial x_i \partial x_j}\langle v_i v_j v_l F_{CE}\rangle\Delta t^2 = \left(\frac{1}{2}\lambda\Delta(\rho u_l) + \lambda\frac{\partial}{\partial x_l}\mathrm{div}(\rho\mathbf{u})\right)\Delta t.$$

According to (44), the fourth order moment leads to

$$-\frac{1}{6}\frac{\partial^3}{\partial x_i \partial x_j \partial x_k}\langle v_i v_j v_k v_l F_{CE}\rangle\Delta t^3 = -\frac{\lambda^2}{2}\frac{\partial}{\partial x_l}\Delta\rho\Delta t + \mathcal{O}\left(\frac{\Delta t^3}{\mathrm{Ma}^2}\right)$$

and fifth order moments are negligible since

$$\langle v_i v_j v_k v_l v_m F_{CE}\rangle\Delta t^4 = \mathcal{O}\left(\frac{\Delta t^4}{\mathrm{Ma}^4}\right)=\mathcal{O}(\Delta t^2).$$

Thus

$$\rho^1 u_l^1 = \rho u_l + \left(\frac{1}{2}\lambda\Delta(\rho u_l) + \lambda \frac{\partial}{\partial x_l}\mathrm{div}(\rho \mathbf{u}) - \frac{\lambda^2}{2}\frac{\partial}{\partial x_l}\Delta\rho - \frac{\partial}{\partial x_i}(\rho u_l u_i) - \frac{1}{\mathrm{Ma}^2}\frac{\partial \rho}{\partial x_l} + \frac{1}{\mathrm{Re}}\frac{\partial}{\partial x_i}(2\rho S_{il}) + \frac{1}{\mathrm{Re}}\frac{\partial}{\partial x_l}\left(\rho \frac{\partial u_i}{\partial x_i}\right)\right)\Delta t + \mathcal{O}(\Delta t^2). \tag{47}$$

Since we assume that all appearing quantities are scaled, the equation for $\rho^1 \mathbf{u}^1$ can only be balanced if $\partial\rho/\partial x_l = \mathcal{O}(\mathrm{Ma}^2)$. Hence, we assume that $\rho = \bar{\rho}(1 + \mathrm{Ma}^2 p)$ for some constant $\bar{\rho} > 0$ and a function p which is assumed to be of order one together with its derivatives in the limit under consideration. (This is the standard scaling of the density in isothermal, low Mach number flows.) Using the additional information on ρ and observing that $\mathrm{Ma}^2 = \mathcal{O}(\Delta t)$, we can simplify (46) in lowest order to

$$\mathrm{div}\,\mathbf{u} = \mathcal{O}(\Delta t). \tag{48}$$

This equation has to be understood in the sense that the order one assumption on $\mathbf{u}$ and p is only consistent if the divergence of $\mathbf{u}$ is $\mathcal{O}(\Delta t)$. Before we explain how the kinetic scheme guarantees the approximate divergence-free condition, we note that relation (48) and the structure of ρ reduces (47) to the Navier–Stokes equation with a first order error term

$$\frac{\partial \mathbf{u}}{\partial t} + (\mathbf{u}\cdot\nabla)\mathbf{u} + \nabla p = \left(\frac{1}{\mathrm{Re}} + \frac{1}{2}\lambda\right)\Delta\mathbf{u} + \mathcal{O}(\Delta t). \tag{49}$$

To explain the mechanism that leads to (48), we use (46) again, keeping the first order terms. After division by Δt and Ma^2 this leads to

$$\frac{\partial p}{\partial t} + \mathrm{div}(p\mathbf{u}) + \frac{1}{\mathrm{Ma}^2}\mathrm{div}\,\mathbf{u} = \frac{1}{2}\lambda\Delta p + \mathcal{O}\left(\frac{\Delta t^2}{\Delta t \mathrm{Ma}^2}\right).$$

To resolve the additional terms of order one on the right hand side, we have to expand (45) one order higher. Using the explicit knowledge of the relevant moments, relation (48), and our assumption on ρ, we find

$$\frac{\partial p}{\partial t} + (\mathbf{u}\cdot\nabla)p + \frac{1}{\mathrm{Ma}^2}\mathrm{div}\,\mathbf{u} = \frac{1}{2}\lambda\Delta p + \mathrm{div}((\mathbf{u}\cdot\nabla)\mathbf{u}) + \mathcal{O}(\Delta t).$$

Note that equations of this type are used in *pseudo-compressibility methods* [47, 48] to ensure the divergence free condition. In fact, it uses elements of Chorin's *artificial compressibility method* [49] to replace $\mathrm{div}\,\mathbf{u} = 0$ by the equation

$$\epsilon\frac{\partial p}{\partial t} + \mathrm{div}\,\mathbf{u} = 0$$

and of the pressure stabilization method

$$\mathrm{div}\,\mathbf{u} - \epsilon\Delta p = 0$$

which was originally used by Hughes *et al*. [50]. However, the convection term and the nonlinear term which follow automatically from the kinetic approach are usually not considered. We thus conclude that *in the coupled limit* $\Delta t, \mathrm{Ma} \to 0$ *with* $\Delta t/\mathrm{Ma}^2 = \lambda$ *with the assumption that* $\rho = \bar{\rho}(1 + \mathrm{Ma}^2 p)$ *and that* $\mathbf{u}$, p *and their derivatives are order one functions, the kinetic scheme is consistent to the incompressible Navier–Stokes equation with effective Reynolds number*

$$\frac{1}{\mathrm{Re}'} = \frac{1}{\mathrm{Re}} + \frac{\lambda}{2}.$$

The scheme can be viewed as a new pseudo-compressibility method.

Note that in the case $\mathrm{Re} = \infty$, the Chapman–Enskog distribution reduces to a Maxwellian and the kinetic scheme is equivalent to the lattice Boltzmann method with relaxation parameter $t_R = \Delta t$. Therefore, LBM can also be viewed as a pseudo-compressibility method in that case. Since an additional viscosity term appears in the coupled limit $\Delta t, \mathrm{Ma} \to 0$, the kinetic scheme with $\nu = 0$ still approximates the solution of an incompressible Navier–Stokes equation. As already mentioned earlier, this idea has been used in [38] to construct Navier–Stokes solutions with a kinetic scheme which is just based on a discrete Maxwellian.

5. NUMERICAL RESULTS AND DISCUSSIONS

We first note that the term involving $\operatorname{div} \mathbf{u}$ in the Chapman–Enskog distribution (32) is actually not important in low Mach number situations and thus can be neglected. Note that such modifications are very simple in the framework of kinetic schemes: by adding or deleting terms in the distribution function, the macroscopic equations can easily be modified. In the case of LBM, on the other hand, the Chapman–Enskog distribution is implicitly given through properties of the collision operator which makes it much harder to develop such schemes for modifications of the incompressible Navier–Stokes equation.

We adjust the viscosity parameter ν in the Chapman–Enskog distribution such that the effective viscosity turns into the required one. This prevents the numerical viscosity from spoiling the results of the simulations. Altogether, we base our kinetic scheme on the following distribution function (which is now written again in unscaled variables)

$$F_{CE,i}(\rho, \mathbf{u}) = F_i^* \rho \left(1 + \frac{\mathbf{u} \cdot \mathbf{v}_i}{c_s^2} - \frac{1}{c_s^2} |\mathbf{u}|^2 + \frac{1}{c_s^4} (\mathbf{u} \cdot \mathbf{v}_i)^2 - \left(\frac{\nu}{c_s^2} - \frac{\Delta t}{2} \right) S : \frac{\mathbf{v}_i \otimes \mathbf{v}_i}{c_s^2} \right).$$

In a first test case, we apply the scheme to a Poiseuille flow in an infinitely long channel (in x_1-direction) of width one with a constant acceleration g. The incompressible Navier–Stokes solution for this case is explicitly known to be

$$u_1(x_2) = \frac{g}{2\nu}(1 - x_2)x_2, \qquad u_2 \equiv 0 \tag{50}$$

with a constant pressure. In our simulation we choose $\rho \equiv 1$ initially. The infinitely long channel is modeled by periodic boundary conditions in the x_1-direction. The fixed wall conditions for $\mathbf{u}$ are enforced simply by setting $\mathbf{u} = \mathbf{0}$ at the boundary nodes. In contrast to LBM, where the no-slip condition has to be enforced by properly setting the incoming occupation numbers, no such complications are found here, because the unknowns in

the kinetic scheme are directly the flow variables ρ and $\mathbf{u}$. The boundary conditions for density can be obtained from the Navier–Stokes equation (28). Multiplying the equation with the outward unit normal vector $\mathbf{n}$ and observing that $\mathbf{u} = \mathbf{0}$ at the boundary, we get the condition

$$c_s^2 \frac{\partial \rho}{\partial \mathbf{n}} = \mathbf{n} \cdot \operatorname{div} \eta. \tag{51}$$

For the exact solution (50) one easily checks that

$$\operatorname{div} \eta = -\nu \rho g \begin{pmatrix} 1 \\ 0 \end{pmatrix}$$

so that $\mathbf{n} \cdot \operatorname{div} \eta = 0$ at the upper and lower walls giving rise to homogeneous boundary conditions for ρ. (According to [47], homogeneous Neumann conditions for ρ are also reasonable in more general, moderate flow situations.) The force term is incorporated into our scheme by a splitting approach: in a first step the kinetic scheme approximates the Navier–Stokes evolution and in a second step, the acceleration is taken care of by an explicit Euler step for the velocity variable. To calculate the stress tensor S, we use central differences.

From the solution (50), we can see that the maximum velocity

$$U = \frac{g}{8\nu}$$

is obtained at the center of the channel. By setting $g = 0.01$ and $\nu = 0.01$, we get $U = 0.125$ (note that U is the Mach number since $c_s = 1$). With 11 points across the channel and initial velocity $\mathbf{u} = \mathbf{0}$, we find a numerical approximation which reproduces the predicted parabolic shape (see Fig. 1). The other velocity component stays zero and the density remains constant. Due to the symmetries in this simple test case, the incompressibility condition is satisfied exactly. Consequently, compressibility errors are not present and the accuracy of the scheme just depends on how closely the steady state is approximated. For several values of t, the $\mathbb{L}^\infty$ error behaves as depicted in Fig. 2. In all calculations, the number of grid points is 11 and $U = 0.125$. The next test case is a slight modification of the previous one, where the top wall of the channel now moves with a fixed velocity w in x_1-direction (Couette flow).

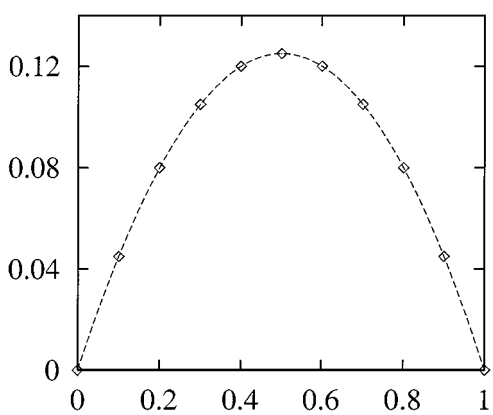

FIG. 1. Poiseuille velocity profile.

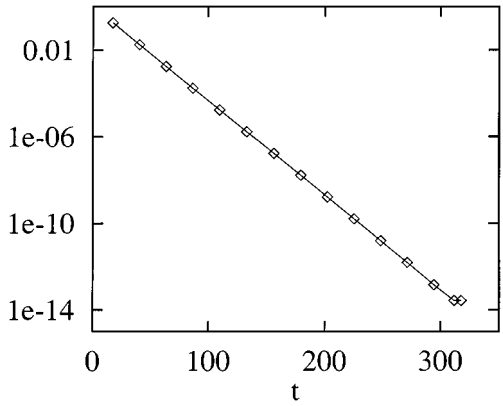

FIG. 2. $\mathbb{L}^\infty$-error versus time.

Here, the exact solution differs from (50) by an additional linear term

$$u_1(x_2) = \frac{g}{2\nu}(1 - x_2)x_2 + wx_2, \qquad u_2 \equiv 0. \tag{52}$$

Again, the **u**-boundary condition at the moving wall is easily enforced by setting $u_1 = w$ and $u_2 = 0$. Using the same settings as above with $w = 0.12$ the results are again in agreement with the exact solution (see Fig. 3). Our final test case is the driven cavity flow problem. The incompressible fluid is now bounded by a square enclosure with side length one. The top lid, which moves with velocity U, generates the fluid motion in the cavity which shows typical vortex phenomena. For our calculations we use a 129×129 uniform grid and Reynolds numbers 100, 400, and 1000. The lid velocity U is set to one and $c_s = 10$ in all cases. The calculations are initialized with $\rho = 1$ and $\mathbf{u} = \mathbf{0}$ inside the cavity. As termination criterion we choose a residue fall of 3.75 decades in the equation for ρ. The typical number of cycles to get steady state solutions is 100,000. We remark that no special attention has been paid to acceleration of convergence. Our aim is only to show that the new discrete velocity method works for complex test problems. (Note that the pressure develops singularities in the top corners due to the jump in the boundary conditions for velocity.) In order to demonstrate

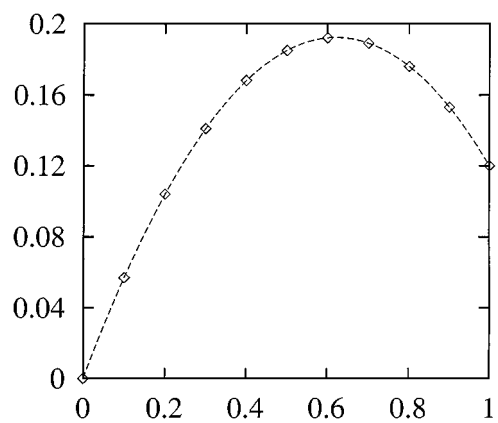

FIG. 3. Velocity profile for Couette flow.

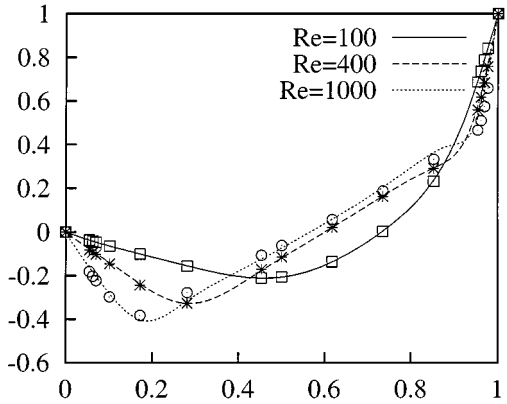

FIG. 4. u_1-velocity along a vertical line through the center of the cavity.

that the kinetic scheme can be used like a lattice Boltzmann method we implement the boundary conditions using the fast *bounce back* algorithm [51]. To explain this approach we remark that on the kinetic level, boundary conditions are required for the transport part of the equation

$$\frac{\partial f}{\partial t} + \mathbf{v} \cdot \nabla f = 0. \tag{53}$$

Since (53) is a linear hyperbolic equation, information has to be provided for those characteristics which enter the domain at a boundary. In our model, the characteristics are straight lines along the discrete velocity directions $\mathbf{v}_1 \cdots \mathbf{v}_8$. The bounce back condition sets the value for the information of an incoming direction equal to the information that leaves the domain in the opposite direction, which is easily available due to the symmetry of the discrete velocity set. It can be shown [51] that these conditions simulate no slip conditions at the Navier–Stokes level. At the upper lid, a modification is required which takes care of the momentum flux generated by the movement [52]. To illustrate our results, the horizontal velocity component u_1 is shown along a vertical section through the center of the cavity (Fig. 4). Similarly, we plot the vertical component u_2 along the central horizontal section

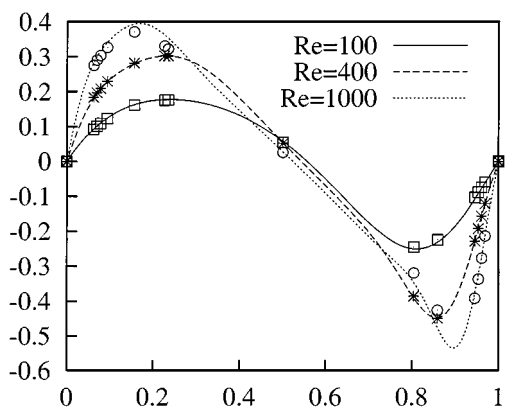

FIG. 5. u_2-velocity along a horizontal line through the center of the cavity.

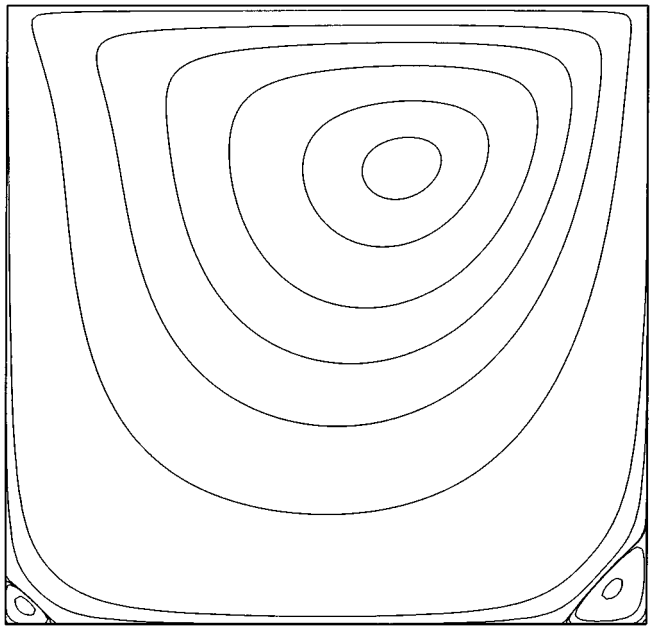

FIG. 6. Re = 100.

(Fig. 5). The results are compared with those obtained by Ghia *et al*. [53] and they are in good agreement. In Figs. 4 and 5, the symbols refer to the tabulated simulation results in [53] and the lines refer to the results obtained by the new kinetic scheme. Plots of the stream functions are given in Figs. 6–8. We remark that the stream function ψ is, strictly speaking, not well defined because the approximate velocity field is not exactly divergence free. In

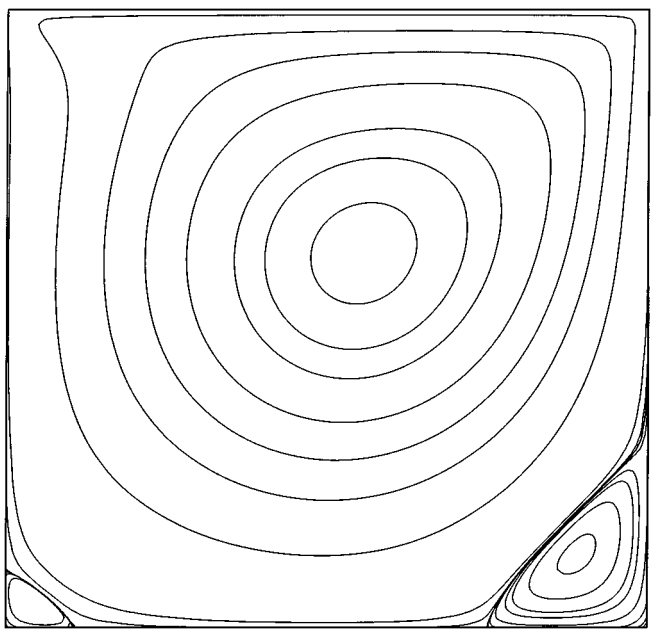

FIG. 7. Re = 400.

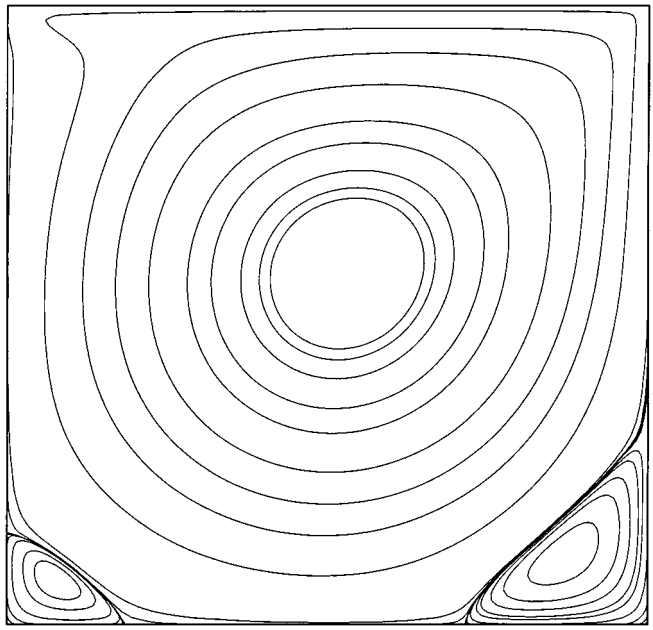

FIG. 8. $\mathrm{Re} = 1000$.

[45], this problem is discussed for the lattice Boltzmann method and we use the proposed numerical procedure for the calculation of ψ (integration of u_2 along horizontal sections from left to right). The levels of the isolines are those from [53]. We limit ourselves in this study to the use of uniform grids, as our purpose is to show that the new discrete velocity method works. With clustered grids, the solution can be different [54]. The numerical cost of the kinetic scheme is directly comparable to that of the lattice Boltzmann method based on the D2Q9 model. Both algorithms have the same structure consisting of a propagation and a collision step. The only difference is that in the kinetic scheme the stress tensor has to be calculated (by taking central differences of the velocity field) and that the equilibrium distribution is extended by the viscosity term. On the other hand, the kinetic scheme needs less memory because there is no need to store the occupation numbers. Apart from two copies of ρ and $\mathbf{u}$ (new and old time step) an efficient implementation requires three more variables to store the stress tensor. Altogether a 2D computation needs nine floating point variables per node, independent of the underlying number of discrete velocities. Compared to that, D2Q9 lattice Boltzmann methods need 21 variables per node (for ρ, $\mathbf{u}$, and two copies of the occupation numbers $f_0, \ldots, f_8$) and the number increases if methods with more velocities are used. Also, when passing over to 3D calculations, the memory usage of the kinetic scheme increases by five variables per site whereas D3Q15 lattice Boltzmann methods need 13 more variables in each node. Of course, the discrepancy becomes even larger if multi-phase flows are simulated. Then, for simple algorithms, the memory requirement has essentially to be multiplied by the number of participating species. Taking these considerations into account, kinetic schemes seem to be a powerful alternative to lattice Boltzmann methods. On the one hand, they are formulated in the same kinetic framework allowing the use of LBM specific solution techniques (kinetic boundary conditions, treatment of phase boundaries in multi-phase flows, etc.). On the other hand, kinetic schemes only use the actual flow variables and thus can profit directly from established finite

difference or finite volume methods. In addition, the memory consumption is greatly reduced compared to lattice Boltzmann algorithms.

Since the idea of LBM is to use a kinetic model which is as simple as possible under the constraint that the macroscopic limit equations are correct, the method is not capable of quantitatively predicting the behavior of a rarefied gas and should therefore only be applied close to equilibrium situations. To show consistency of LBM to the Navier–Stokes equation, exactly this equilibrium assumption is used in the *Chapman–Enskog* expansion which amounts to assuming that the occupation numbers are given by a Chapman–Enskog distribution. A natural idea is therefore to build the Chapman–Enskog distribution directly into the algorithm which is exactly the construction principle of the present kinetic scheme. Thus, kinetic schemes can be viewed as a consequent advancement of the lattice Boltzmann method.

We conclude our discussion with a remark concerning the extension to the full Navier–Stokes system including the energy equation. A fundamental problem of the basic lattice Boltzmann method based on a simple BGK collision operator is that the Prandtl number is not a free parameter. In a kinetic scheme, the heat conduction and viscosity parameters enter directly into the Chapman–Enskog distribution (similar to the continuous case (27)) and thus can naturally be varied independently.

6. CONCLUSIONS

The similarities and differences between the lattice Boltzmann method, which has recently become popular, and the kinetic schemes, which are routinely used in computational fluid dynamics, are studied. A new discrete velocity method for the numerical simulation of incompressible Navier–Stokes equations is presented by combining both the approaches. This approach of kinetic schemes with discrete distributions is shown to be more convenient and useful compared to the lattice Boltzmann method. Since both methods coincide for a particular choice of parameters, the analysis of the kinetic scheme also applies directly to LBM in that case. In particular, the conclusion that the kinetic scheme is a special pseudo-compressibility method illuminates the lattice Boltzmann approach.

REFERENCES

1. G. R. McNamara and G. Zanetti, Use of the Boltzmann equation to simulate lattice-gas automata, *Phys. Rev. Lett.* **61**, 2332 (1988).
2. U. Frisch, D. d'Humières, B. Hasslacher, P. Lallemand, Y. Pomeau, and J.-P. Rivet, Lattice gas hydrodynamics in two and three dimensions, in *Complex Systems*, Vol. 1, p. 649; reprinted in *Lattice Gas Methods for Partical Differential Equations*, edited by Doolen *et al*. (Addison–Wesley, Reading, MA, 1990), p. 75.
3. D. H. Rothman and S. Zaleski, Lattice-gas models of phase separation: Interfaces, phase transitions and multi-phase flow, *Rev. Mod. Phys.* **66**(4), 1417 (1994).
4. D. H. Rothman and S. Zaleski, *Lattice–Gas Cellular Automata: Simple Models of Complex Hydrodynamics* (Cambridge Univ. Press, Cambridge, UK, 1997).
5. R. Benzi, S. Succi, and M. Vergassola, The lattice Boltzmann equation: Theory and applications, *Phys. Rep.* **222**(3), 145 (1992).
6. S. Chen and G. D. Doolen, lattice Boltzmann method for fluid flows, *Ann. Rev. Fluid Mech.* **30**, 329 (1998).
7. T. Platkowski and R. Illner, Discrete Velocity models of the Boltzmann equation: A survey on the mathematical aspects of the theory, *SIAM Rev.* **30**, 213 (1988).

8. X. He and L.-S. Luo, Theory of the lattice Boltzmann method: From the Boltzmann equation to the lattice Boltzmann equation, *Phys. Rev. E* **56**(6), 6811 (1997).
9. N. Cao, S. Chen, S. Jin, and D. Martinez, Physical symmetry and lattice symmetry in the lattice Boltzmann method, *Phys. Rev. E* **55**(1), 21 (1997).
10. S. M. Deshpande, Kinetic flux splitting schemes, in *Computational Fluid Dynamics Review 1995: A State-of-the-Art Reference to the Latest Developments in CFD*, edited by M. M. Hafez and K. Oshima (Wiley, New York, 1995).
11. R. H. Sanders and K. H. Prendergast, On the origin of the 3-kiloparsec arm, *Astrophys. J.* **188**, 489 (1974).
12. A. Harten, P. D. Lax, and B. van Leer, On upstream differencing and Godunov-type schemes for hyperbolic conservation laws, *SIAM Rev.* **25**, 35 (1983).
13. D. I. Pullin, Direct simulation methods for compressible inviscid ideal-gas flow, *J. Comput. Phys.* **34**, 231 (1980).
14. R. D. Reitz, One-dimensional compressible gas dynamic calculations using the Boltzmann equation, *J. Comput. Phys.* **42**, 108 (1981).
15. S. M. Deshpande, *A Second-Order Accurate Kinetic Theory Based Method for Inviscid Compressible Flows*, NASA TP 2613, 1986.
16. S. M. Deshpande, *Kinetic Theory Based New Upwind Methods for Inviscid Compressible Flows*, AIAA Paper 86-0275, American Institute of Aeronautics and Astronautics, New York, 1986.
17. J. C. Mandal and S. M. Deshpande, Kinetic flux vector splitting for Euler equations, *Comput. & Fluids* **23**(2), 447 (1993).
18. B. Perthame, Boltzmann-type schemes for gas dynamics and the entropy property, *SIAM J. Numer. Anal.* **27**(6), 1405 (1991).
19. F. Coron and B. Perthame, Numerical passage from kinetic to fluid equations, *SIAM J. Numer. Anal.* **28**, 26 (1991).
20. K. H. Prendergast and Kun Xu, Numerical hydrodynamics from gas-kinetic theory, *J. Comput. Phys.* **109**, 53 (1993).
21. K. Xu, L. Martinelli, and A. Jameson, Gas-kinetic finite volume methods, flux-vector splitting and artificial diffusion, *J. Comput. Phys.* **120**, 48 (1995).
22. S. V. Raghurama Rao and S. M. Deshpande, Peculiar velocity based upwind method for inviscid compressible flows, *Comput. Fluid Dynam. J.* **3**(4), 415 (1995).
23. S. V. Raghurama Rao, Peculiar velocity based upwind method for inviscid compressible flows, in *Lecture Notes in Physics* (Springer-Verlag, Berlin, 1995), Vol. 453, p. 112.
24. S. Kaniel, Approximation of the hydrodynamic equations by a transport process, in *Proceedings of IUTAM Symposium on Approximation Methods for Navier–Stokes Problems*, Lecture Notes in Math., edited by R. Rautmann (Springer-Verlag, Berlin/New York, 1980), Vol. 771.
25. S. Kaniel, A kinetic model for the compressible flow equation, *Indiana Univ. Math. J.* **37**(3), (1988).
26. M. Junk, *Kinetic Schemes: A New Approach and Applications*, Ph.D. thesis, Universität Kaiserslautern, Shaker Verlag, 1997.
27. B. Perthame, Second-order Boltzmann schemes for compressible Euler equations in one and two space dimensions, *SIAM J. Numer. Anal.* **29**(1), 1 (1992).
28. S. Y. Chou and D. Baganoff, Kinetic flux vector splitting for the Navier–Stokes equations, *J. Comput. Phys.* **130**, 217 (1997).
29. B. Manoj Kumar, S. V. Raghurama Rao, R. Balasubramanyam, and S. M. Deshpande, *Kinetic Flux Vector Splitting for Navier–Stokes Equations Based on Chapman–Enskog Distribution*, Fluid Mechanics Reports, 97 FM 9, Department of Aerospace Engineering, Indian Institute of Science, Bangalore, India, 1997.
30. S. Ramanan, S. V. Raghurama Rao, and S. M. Deshpande, *Peculiar Velocity and Chapman–Enskog Distribution Function Based Upwind Method (PVU-CE) for Navier–Stokes Equations*, Fluid Mechanics Reports, FM 98 4, Department of Aerospace Engineering, Indian Institute of Science, Bangalore, India, 1998.
31. K. Xu and K. H. Prendergast, Numerical Navier–Stokes solutions from gas-kinetic theory, *J. Comput. Phys.* **114**, 9 (1994).

32. M. Bäcker and K. Dressler, A kinetic method for strictly nonlinear scalar conservation laws, *Z. Angew. Math. Phys.* **42** (1991).
33. Y. Giga and T. Miyakawa, A kinetic construction of global solutions of first order quasilinear equations, *Duke Math. J.* **50**, 505 (1983).
34. B. Perthame and E. Tadmor, A kinetic equation with kinetic entropy functions for scalar conservation laws, *Comm. Math. Phys.* **136**, 501 (1991).
35. P. L. Lions, B. Perthame, and E. Tadmor, A kinetic formulation of multidimensional scalar conservation laws and related equations, *J. Am. Math. Soc.* **7**, 169 (1994).
36. B. T. Nadiga and D. I. Pullin, A method for near-equilibrium discrete velocity gas flows, *J. Comput. Phys.* **112**, 162 (1994).
37. M. Junk, *On the Construction of Discrete Equilibrium Distributions for Kinetic Schemes*, ITWM Report, Institut für Techno- und Wirtschaftsmathematik, Kaiserslautern, Germany, 1998.
38. M. Junk, Kinetic schemes in the case of low Mach numbers, *J. Comput. Phys.* **151**, 947 (1999).
39. S. Chen, H. Chen, and W. H. Matthaeus, Recovery of the Navier–Stokes equations using a lattice-gas Boltzmann method, *Phys. Rev. A* **45**, 5339 (1992).
40. Y. H. Qian, D. D'Humières, and P. Lallemand, Lattice BGK models for Navier–Stokes equation, *Europhys. Lett.* **17**(6), 479 (1992).
41. J. Huang, F. Xu, M. Vallieres, D. H. Feng, Y. H. Qian, B. Fryxell, and M. R. Strayer, A thermal LBGK model for large density and temperature differences, *Int. J. Mod. Phys. C* **8**, 827 (1997).
42. W. G. Vincenti and C. H. Kruger, Jr., *Introduction to Physical Gas Dynamics* (Wiley, New York, 1965).
43. K. Huang, *Statistical Mechanics* (Wiley, New York, 1987).
44. M. N. Kogan, *Rarefied Gas Dynamics* (Plenum, New York, 1969).
45. S. Hou, Q. Zou, S. Chen, G. Doolen, and A. C. Cogely, Simulation of cavity flow by the lattice Boltzmann method, *J. Comput. Phys.* **118**, 329 (1995).
46. S. V. Raghurama Rao and M. Junk, *A Discrete Velocity Method with Chapman–Enskog Distribution*, paper in preparation.
47. C. Hirsch, *Numerical Computaion of Internal and External Flows* (Wiley, New York, 1990), Vol. 2.
48. R. Rannacher, On Chorin's projection method for the incopressible Navier–Stokes equations, in *Lecture Notes in Mathematics* (Springer-Verlag, New York/Berlin, 1992), Vol. 1530.
49. A. J. Chorin, A numerical method for solving incompressible viscous flow problems, *J. Comput. Phys.* **2**, 12 (1967).
50. T. J. R. Hughes, L. P. Franca, and M. Balestra, A new finite element formulation for computational fluid mechanics. V. Circumventing the Babuska–Brezzi condition: A stable Petrov–Galerkin formulation of the Stokes problem accomodating equal order interpolation, *Comput. Methods Appl. Mech. Eng.* **59**, 85 (1986).
51. R. Cornubert, D. d'Humieres, and D. Levermore, A Kundsen layer theory for lattice gases, *Phys. D* **47**, 241 (1991).
52. A. Ladd, Numerical simulations of particulate suspensions via a discretized Boltzmann equation. Part 1. Theoretical foundation, *J. Fluid Mech.* **271**, 285 (1994).
53. U. Ghia, K. N. Ghia, and C. T. Shin, High-Re solutions for incompressible flow using the Navier–Stokes equations and a multigrid method, *J. Comput. Phys.* **48**, 387 (1982).
54. S. Sundaresan, S. Nagarajan, S. M. Deshpande, and R. Narasimha, 2-D Lid-driven cavity flow at high Reynolds numbers: Some interesting fluid-dynamical issues, in *16th International Conference on Numerical Methods in Fluid Dynamics, Arcachon, France, July 6–10, 1998*, Lecture Notes in Physics (Springer-Verlag, New York/Berlin), Vol. 515.